Anthracene–BODIPY Cassettes: Syntheses and Energy Transfer

Chi-Wai Wan,[a] Armin Burghart,[a] Jiong Chen,[a] Fredrik Bergström,[b] Lennart B.-Å. Johansson,[b] Matthew F. Wolford,[c] Taeg Gyum Kim,[c] Michael R. Topp,[c] Robin M. Hochstrasser,[c] and Kevin Burgess*[a]

Abstract: Compounds based on the 4,4-difluoro-1,3,5,7-tetramethyl-4-bora-3a,4a-diaza-*s*-indacene (BODIPY) framework are excellent fluorescent markers. When BODIPY dyes of this type are conjugated to functionalities that absorb at relatively short wavelengths, those functionalities can, in some molecules, transmit the absorbed energy to the BODIPY which then fluoresces. In such cases the BODIPY fragment acts as an acceptor while the other group serves as a donor. Energy transfer efficiencies in such donor–acceptor cassette systems must vary with the relative orientation of the two components, and with the structure of the linkers that attach them. This study was designed to probe these issues for the special case in which the linkers between the donor and acceptor fragments are conjugated. To do this, the cassettes **3**–**10** were prepared. Electrochemical studies were performed to provide insight into the degree of donor–acceptor conjugation in these systems. X-ray Crystallographic studies on single crystals of compounds **7** and **9** revealed the favored conformations of the donor and acceptor fragments in the solid state. Absorption, fluorescence, and time-resolved fluorescence spectra of the compounds were recorded, and quantum yields for the cassettes excited at the donor λ_{max} were measured. Fluorescence steady-state anisotropy data were determined for cassettes **3** and **9** to provide information about the mutual direction of the transition dipole moments.

Keywords: dyes/pigments · energy transfer · fluorescent probes · UV/Vis spectroscopy

Introduction

Fluorescent labels that emit light at wavelengths distant from that of the source used to excite them have many applications in biotechnology. For single dye systems the difference between the S_0 absorption and the S_1 emission wavelengths is the Stokes' shift.[1] When the Stokes' shift of a single dye is insufficient for a particular application, strategies that exploit through-space energy transfer between two dyes are frequently used.[2, 3] An absorbing molecular fragment (a donor) is arranged to be proximal to an emitting fragment (an acceptor); the donor is then excited at wavelengths close to its λ_{max}, and the fluorescence of the acceptor is observed. For biotechnological applications, the donor and acceptor units are usually connected via non-conjugated linker systems, hence the predominant energy transfer mechanism is through-space (usually Förster mechanism; Figure 1a).[4] A requirement for Förster energy transfer is that the emission spectrum of the donor must overlap with the absorption spectrum of the acceptor. That requirement places an upper limit on the range of fluorescence wavelengths from two-dye cassettes irradiated using a single excitation wavelength.

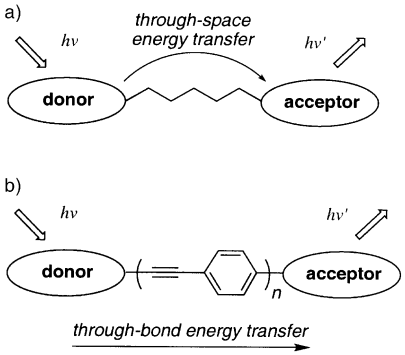

Figure 1. Through-space and through-bond energy transfer.

[a] Prof. K. Burgess, Dr. C.-W. Wan, Dr. A. Burghart, Dr. J. Chen
Texas A & M University, Chemistry Department
P.O. Box 30012, College Station, Texas 77842 (USA)
E-mail: burgess@tamu.edu

[b] F. Bergström, Prof. L. B.-Å. Johansson
Department of Chemistry: Biophysical Chemistry
Umeå University, 90187 Umeå (Sweden)

[c] Dr. M. F. Wolford, Dr. T. G. Kim, Prof. M. R. Topp, Prof. R. M. Hochstrasser
Department of Chemistry, University of Pennsylvania
Philadelphia, PA 19104 (USA)

DOI: 10.1002/chem.200304754

In contrast to through-space energy transfer cassettes, donor and acceptor units connected by *conjugated* linker fragments may transfer energy via several pathways. These include through-space energy transfer, but also other pathways that may be collectively referred to as through-bond energy transfer mechanisms (Figure 1b), which include Dexter energy transfer and others.[5] The literature on molecules that exhibit through-bond energy transfer may be divided into that which deals with oligomeric conjugated materials,[6] and other contributions featuring models for biological systems (e.g. porphyrin-containing systems).[7–11] Energy transfer through bonds does *not* require the emission spectrum of the donor to overlap with the lowest energy excited states of the acceptor. Of course, excitation of any molecule above the S_1 state will lead to S_1 to S_0 fluorescence, but the higher energy absorption cross sections are often low and they vary considerably between molecules. In conjugated donor–acceptor cassettes, however, a given donor part can be incorporated to absorb strongly at a given wavelength, and the acceptors can be varied to emit at different wavelengths that are distant from that of the source used to excite them. We are interested in designing fluorescent dyes for biotechnology that exploit this phenomenon.[12, 13]

For conjugated cassettes of the type shown in Figure 1b, it may not be possible to ascertain how much energy transfer proceeds via through-bond mechanisms relative to the through-space pathways. This is very likely to be the case when the donor and acceptor fragments are relatively close together. Nevertheless, the overall rates of energy transfer can be measured; they in turn will be influenced by the structure of the donor, acceptor, and linker fragments, and the orientation of the donor–linker–acceptor connectivity.

The work described herein focuses on the last of the issues outlined above: overall rates of energy transfer in donor–acceptor cassettes as a function of the linker structure and orientation. To do this, compounds **1** and **2** were used as mimics of the donor and acceptor fragments in cassettes **3**–**10**; all of which feature dyes of the BODIPY type as acceptors.[7, 14, 15] The structures of these cassettes were determined in part by synthetic accessibility. For instance, it is much easier to prepare molecules with aryl substituents at C^8 of the BODIPY framework, than with alkyne groups there, but it is relatively straightforward to put either type of substituent at C^4. Another consideration in the design of cassettes **3**–**10** was future applications of these materials. Thus, in molecules **4**–**6** a bromine is included to allow these cassettes to be attached to other molecules via organometallic coupling reactions. Spectroscopically, the bromine substituent is unlikely to have any appreciable effect, and comparisons between cassettes **3** and **4** allow this assumption to be explored in one representative case.

Efficiencies of energy transfer in a conjugated donor–acceptor cassettes must depend on the orientation of the donor and acceptor fragments (a key factor for Förster transfer),[16] and the nature of the π-system that connects them (particularly relevant to through-bond transfer mechanisms). The work that is described here features several derivatives of BODIPY **2** which were investigated to explore some of these orientation/connection issues. Specifically, compounds **3**–**6**, each having an anthracene donor connected to the side of a BODIPY fragment via different linkers, and the "axially-linked" systems **7**–**10** were compared. Absorption and fluorescence emission data collected for these compounds were interfaced with results from X-ray crystallographic, electrochemical, and time resolved fluorescence experiments to begin to understand how the structure and electronic properties of these molecules correlate with their spectroscopic characteristics.

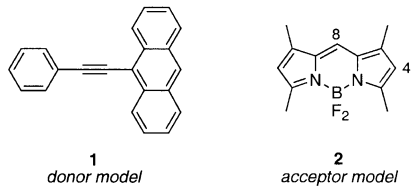

1 *donor model*

2 *acceptor model*

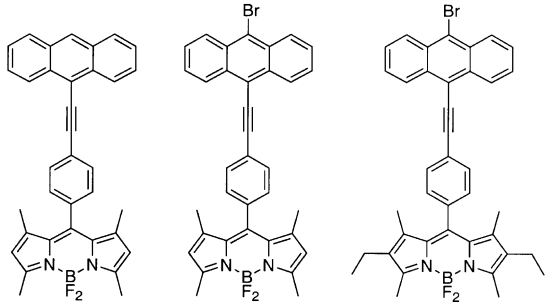

3 **4** **5**

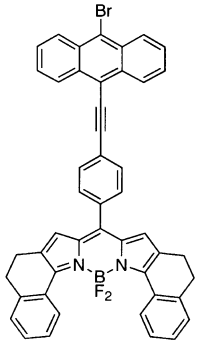

6

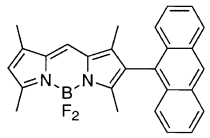

7

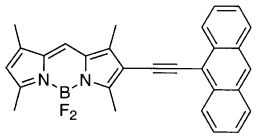

8

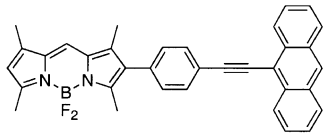

9

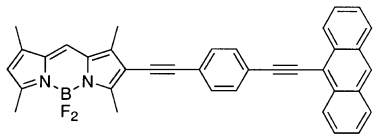

10

Results and Discussion

Syntheses of the cassettes: Anthracene derivative **1** was prepared via the Sonogashira coupling shown in Scheme 1; this was the key reaction used for most of the syntheses of the cassettes described here. Thus cassette **3** was prepared via similar coupling of the alkyne-functionalized BODIPY.[13] Cassettes **5**, **6**, and **7**, were prepared in the same way, but beginning with starting materials for which syntheses have been reported by this group before.[12, 13, 17]

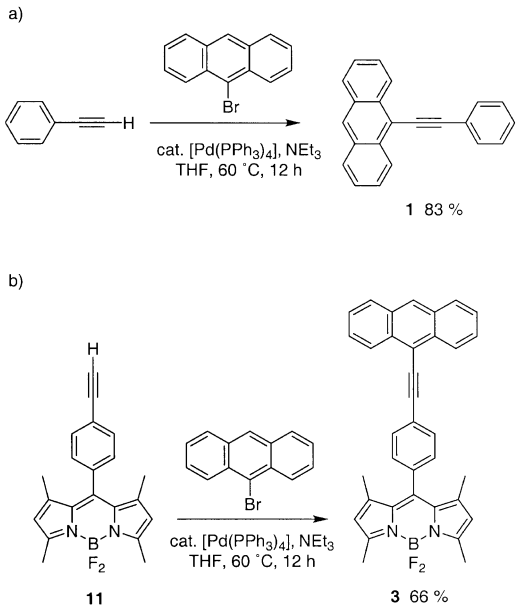

Scheme 1. Preparation of compounds **1** and **3**.

Cassette **7** was prepared by the sequence in Scheme 2a beginning with commercially available 3,5-dimethylpyrrole-2-carbaldehyde. Iodination, under basic conditions, gave the 4-iodo derivative **12**, and this was then condensed with 2,4-dimethylpyrrole and treated with boron trifluoride to give the BODIPY **13**. Suzuki coupling[18] of **13** to the 9-anthracenyl boronic acid gave the desired cassette **7**.

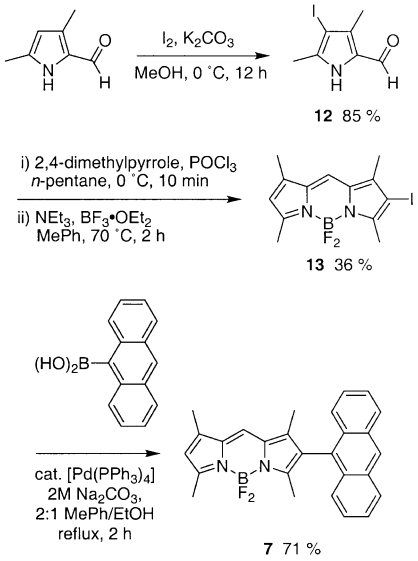

Scheme 2a. Preparation of cassette **7**.

Cassette **8** was also prepared via a route that involved the iodo-BODIPY **13** (Scheme 2b). Successive Sonogashira couplings[19, 20] of this with trimethylsilylacteylene and with 9-bromoanthracene gave the desired product. Possibly the most difficult step to develop in this synthesis was the removal of the trimethylsilyl group, because the BODIPY frameworks are not stable to prolonged treatment with fluoride ion. This transformation was accomplished by careful control of the reaction temperature and time.

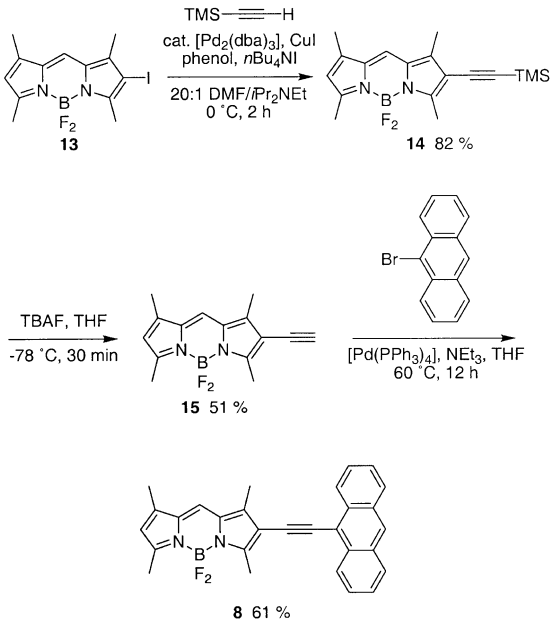

Scheme 2b. Preparation of cassette **8**.

Scheme 2c outlines the synthesis devised for dye **9**. This features a Suzuki, silyl deprotection, Sonogashira sequence. Similarly, cassette **10** was prepared by a Sonogashira, silyl-deprotection, Sonogashira sequence as shown in Scheme 2d involving compound **19**.[13]

Cyclic voltammetry: Redox potential data can be related the electronic conjugation of the chromophores within the cassettes, hence the cassettes **3** and **7**–**10** were studied by cyclic voltammetry. The single chromophore models **1** and **2** were also studied to provide references for the various molecular components. Table 1 summarizes the data obtained (throughout these experiments, chloroform solvent was used and the scan rate was 100 mV s^{-1}).

All compounds exhibited irreversible redox waves, with the exception of the reduction waves of **2** and **7** for which the waves are partially reversible. For cassettes **3**, **7**, **9**, **10** it was shown that two electrons could be removed from (and added to) the system. Those electron transfer steps are most likely related to redox events on the chromophore parts of the molecules. The oxidation potentials of the model dyes **1** and **2** were almost the same (0.85 and 0.88 V, respectively), so that in the cassettes the oxidation steps corresponding to the anthracene and to the BODIPY, respectively, coalesced.

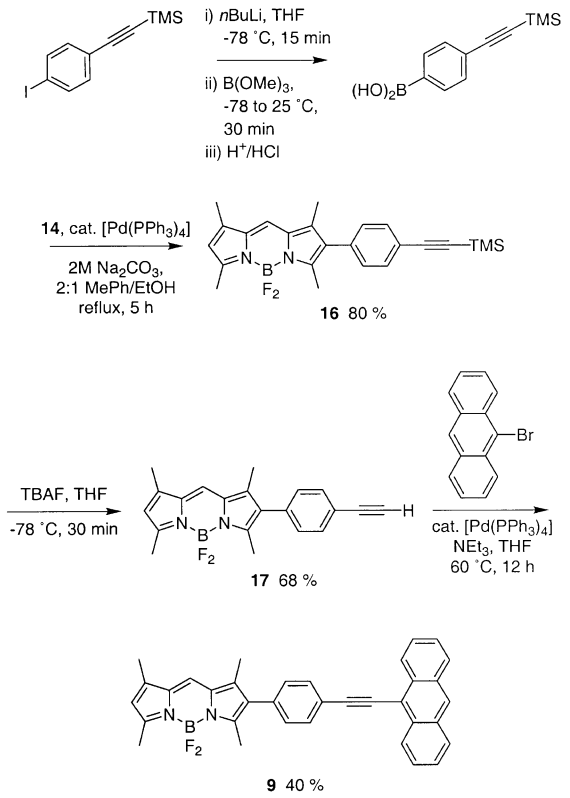

Scheme 2c. Preparation of cassette **9**.

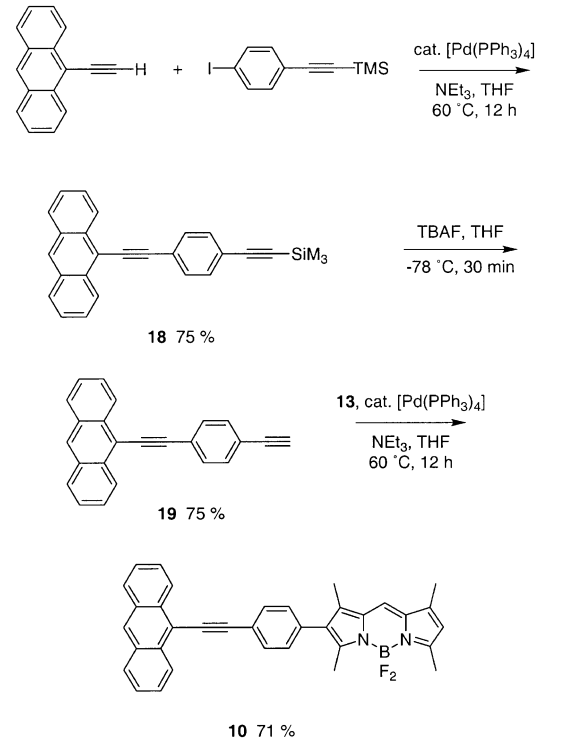

Scheme 2d. Preparation of cassette **10**.

Conversely, reduction gave two distinct waves, at least for compounds **3**, **9**, and **10** and the reduction potential data was useful for probing the π-conjugation in the systems. For model **1**, the redox wave is beyond the accessible range (< -2.50 V). This anthracene reduction is also not visible for **7**, only the BODIPY reduction at -1.71 V was observed. This potential is the most negative of those measured for **3**, **7**–**10** hence this cassette is the one that showed the least conjugation within the series. Compounds **3** and **9**, which possess the same linker, display some small degree of conjugation because their reduction potentials corresponding to the BODIPY fragment are less negative (-1.66 and -1.69 V, respectively) than for **2** and **7**. Moreover, the reduction corresponding to the anthracene part of **3** and **9** occurred in the observable range (≈ -2.2 V); this also indicates that it was more conjugated in these molecules than in compound **2**. These trends were observed to continue for compound **10**, indicating a higher degree of conjugation. Interestingly, the compound **8** was shown to have a relatively low oxidation potential, a modestly negative reduction potential, and no second oxidation or reduction. These electrochemical characteristics are indicative of a well-conjugated system.

Table 1. Redox potentials of compounds **1**–**3** and **7**–**10** in CH_2Cl_2. (Ferrocene was used as internal standard. Scan rate 100 mV s^{-1}.)

Compound	Oxidation potentials E_{pa} [V]	Reduction potentials E_{pc} [V]
1	+0.88	--[a]
2	+0.85	−1.75 ($E_{1/2} = -1.66$ V, $i_{pa}/i_{pc} = 0.20$)
3	+0.85 (2 e)	−1.69 2nd wave: −2.21
7	+0.80 (2 e)	−1.71 ($E_{1/2} = -1.65$ V, $i_{pa}/i_{pc} = 0.22$)
8	+0.58	−1.54
9	+0.85 (2 e)	−1.66 2nd wave: −2.26
10	+0.83 (2 e)	−1.57 2nd wave: −2.20

[a] Redox wave not accessible under conditions employed.

The data described above indicate increasing conjugation in the series **7** < **9** and **3** < **10** < **8**. This observation is chemically reasonable. Cassette **7**, having a direct connection between the BODIPY and 9-anthracenyl components is likely to adopt a twisted conformation in which two chromophores are electronically independent and therefore less conjugated. The BODIPY-to-benzene connection in cassettes **3** and **9** is also likely to impede conjugation for similar reasons. However, the 1,4-bis(ethynyl)phenyl linker in **10** allows good electronic communication between the dyes, and when the phenyl linker is removed, as in **8**, there is almost no barrier to π-conjugation.

Single crystal X-ray studies: Figure 2 shows representations of compounds **7** and **9** generated from X-ray crystallographic coordinates. The bond lengths and angles are unexceptional for these systems, except that the structures do show the degree of twist between the BODIPY fragment and the peripheral aryl substituent (9-anthracenyl for **9** and a substituted benzene ring for **3**). Inspections of these models shows that the anthracenyl fragment of **7** clearly encounters

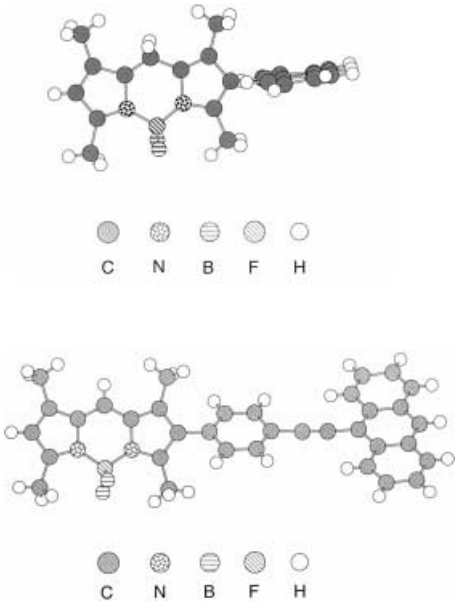

Figure 2. Chem3D diagrams from single crystal X-ray diffraction studies of a) cassette **7**, and b) cassette **9**.

more steric interactions with the BODPY framework than the 1,4-disubstituted phenyl substituent of **9**. Thus the twist between the donor and acceptor planes is more rigidly enforced in **7** than in **9**.

Spectroscopic properties: The absorption spectra of the cassettes in ethanol and chloroform display peaks due to strong and weak $S_0 \rightarrow S_1$ transitions with maxima at 500–645 nm and 365–445 nm, for the BODIPY group and anthracene groups, respectively. A strong higher-energy transition of anthracene was observed at about 265 nm. For the model compound **20**, absorptions are observed at about 300 nm that can be ascribed to the $S_0 \rightarrow S_1$ transition of the conjugated phenylethynyl system; similar absorptions for the cassettes are therefore likely to be due to the phenylethynyl linker system (Figure 3). For most of these samples, the absorption spectrum approximates that which would be expected from adding the components together.

The following experiment was performed to test whether attaching the chromophores causes a weak perturbation of the absorbance for the component parts. The molar absorption at the BODIPY component of the cassette studied most in this paper (see below), cassette **5**, was measured as $40\,000\,\text{M}^{-1}\text{cm}^{-1}$ in $CHCl_3$. The value measured from the absorption spectrum of **5** in Figure 3 is $20\,000\,\text{M}^{-1}\text{cm}^{-1}$ for the absorption in the anthracene region. These values are perfectly consistent with that for anthracene derivatives including, for instance, compound **20** ($30\,000\,\text{M}^{-1}\text{cm}^{-1}$), which is more highly conjugated than the residue used in the cassettes. These data show that attaching the anthracene compenent to the acceptor system causes minimal perturbation of the absorptivity of that component.

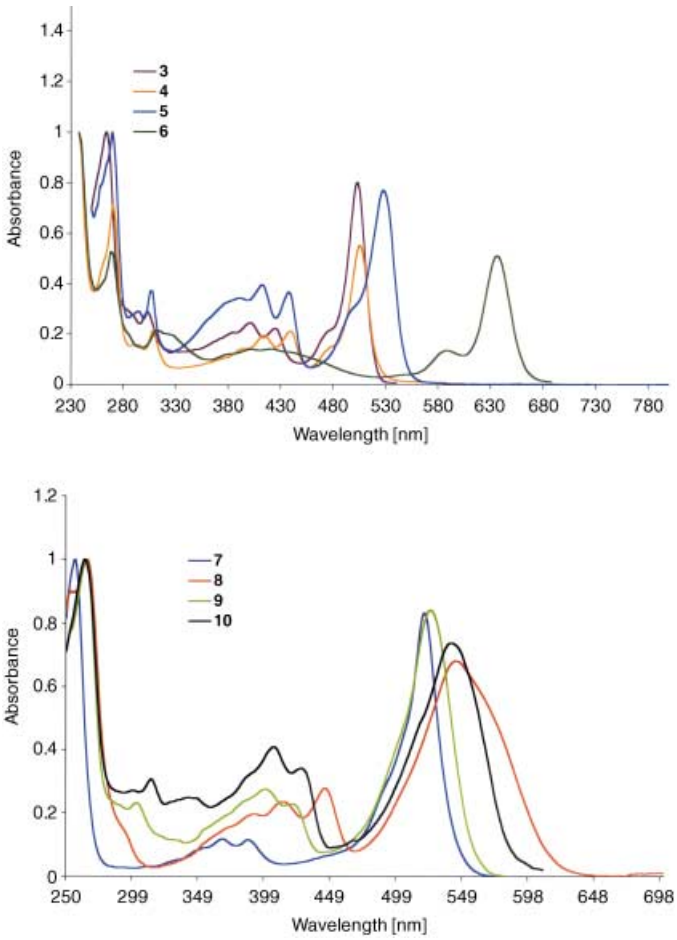

Figure 3. Normalized absorption spectra of a) cassettes **3**–**6** and b) **7**–**10** in $CHCl_3$.

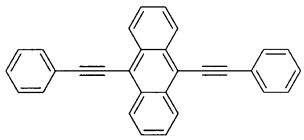

20

Compound **8** does not have a sterically enforced twist to prevent the donor and acceptor coming into a planar conformation. Consequently, the absorption spectrum for this compound differs slightly from the others, but perhaps not as much as might be expected. The absorption maximum for cassette **8** is red-shifted by about 40 nm compared with **9**, **10**, **3** where the linker is a phenylethynyl group. These shifts agree qualitatively with that between anthracene and 9,10-bis(phenylethynyl)anthracene (BPEA) **20**.[21]

Comparisons of the absorption spectra of the acceptor components may use cassette **3** as a reference point since its $\lambda_{max\,abs}$ closely resembles that of the free BODIPY **2** (500 and 504 nm when dissolved in ethanol and chloroform, respectively). For cassettes **7** and **9**, in which the short edge of the acceptor (i.e., C^2) is directly bound to an aromatic group, the $\lambda_{max\,abs}$ values are red-shifted by about 20 nm compared with **3**. Cassettes **8** and **10**, where the immediate linkage is to an ethynyl group, have $\lambda_{max\,abs}$ values red-shifted by about 40 nm

compared with **3**. Furthermore, the spectral band shape of the cassettes **7**–**10** are broader than **3**. All cassettes show a modest solvent dependence with a few nanometers blue-shift upon replacing the solvent ethanol with chloroform.

The fluorescence emission spectra of the cassettes show maxima varying between 515 and 650 nm (Figure 4). The shift between fluorescence and absorption maxima is between

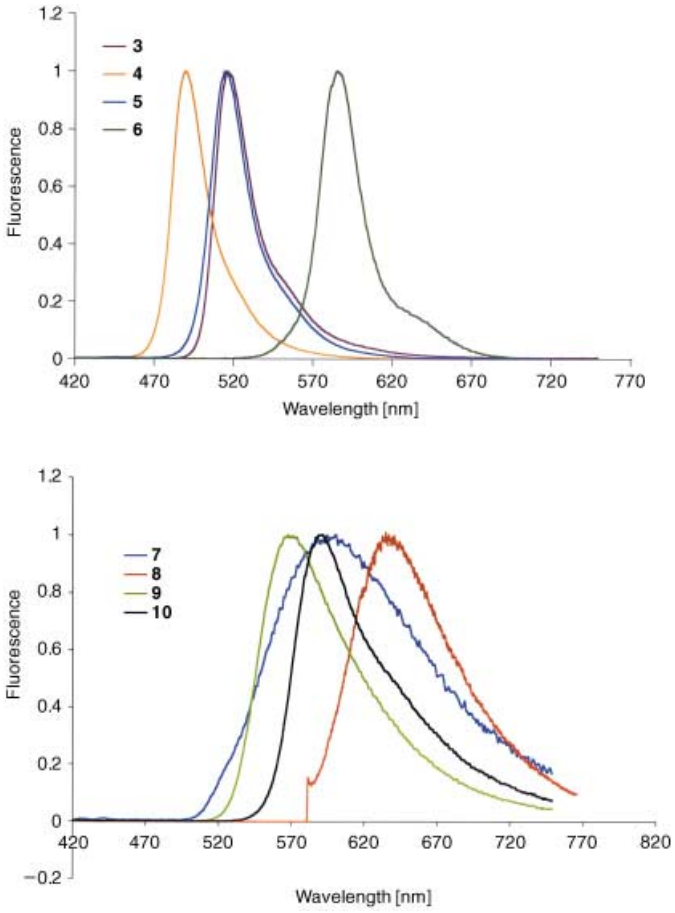

Figure 4. Corrected normalized fluorescence emission spectra of a) compounds **3**–**6** and b) **7**–**10** in $CHCl_3$.

5500–11000 cm^{-1}, when the cassettes are excited at the $S_0 \rightarrow S_1$ transition of the donor. The corresponding difference is 18400–23300 cm^{-1} when the donor is excited at the $S_0 \rightarrow S_2$ transition. The spectral band shapes of the cassettes are similar to those of parent BODIPY **2**, although somewhat broader. Cassettes **9** and **3**, which only differ in linker attachment site on the BODIPY group, have very different spectra. The spectrum of **3** much resembles that of BODIPY **2**, while the spectrum of **9** is considerably shifted to the red with a fluorescence maximum at 569 nm. This difference may be due to the fact that substitution at the BODIPY C^2 position lowers the symmetry, and this perturbs the S_0 and S_1 states. In unpublished studies, we have also found a similar red-shift for *N*-(4,4-difluoro-1,3,5,7-tetramethyl-4-bora-3a,4a-diaza-*s*-indacene-2-yl)iodoacetamide, which is also substituted at C^2.[22] The fluorescence from the donors in all the cassettes was very weak, indicating rapid energy transfer from donor to acceptor (the solvents chloroform, ethanol and propane-1,2-diol were tested). Based on lifetime measurements described below, we estimate the donor fluorescence quantum yields in the cassettes to be $< 5 \times 10^{-5}$.

The acceptor fluorescence time profiles of the cassettes appear to be mono-exponential. For example, the acceptor lifetimes of the cassettes in chloroform vary between 0.5 to 4.0 ns (Table 2), and in most cases are significantly longer than when the compounds are dissolved in ethanol (0.13 to 3.2 ns). The shortest lifetimes were measured found for cassette **8**.

Table 2. Absorption and fluorescence spectroscopic properties of compounds **3**, **4**, **7**, **8**, **9**, and **10** in ethanol and chloroform.

Cassette	Solvent	λ_{fl} (S_0^A) nm[a]	D(S_1) – A(S_1) 10^3 cm^{-1}[b]	D(S_2) – A(S_1) 10^3 cm^{-1}[b]	Φ[c]	τ[d] [ns]	ET Effic. [%]
3	EtOH	514	5.6	19.0	0.16 ± 0.04	1.1	> 95
3	$CHCl_3$	517	5.5	18.4	0.39 ± 0.05	2.1	> 95
4	EtOH	541	6.0	19.3	0.57 ± 0.03	4.0	> 95
4	$CHCl_3$	545	5.9	18.8	0.67 ± 0.03	4.0	> 95
7	EtOH	615	11.1	23.3	0.05 ± 0.01	1.0	> 95
7	$CHCl_3$	594	10.3	22.1	0.25 ± 0.02	2.7	> 95
8	EtOH	640	8.8	22.5	0.01 ± 0.01	0.3	> 95
8	$CHCl_3$	647	8.8	22.3	0.02 ± 0.01	0.5	> 95
9	EtOH	568	7.5	20.9	0.28 ± 0.03	1.7	> 95
9	$CHCl_3$	569	7.4	20.2	0.75 ± 0.06	3.7	> 95
10	EtOH	588	7.7	21.5	0.22 ± 0.02	1.3	> 95
10	$CHCl_3$	590	7.6	20.8	0.42 ± 0.03	2.2	> 95

[a] The peak wavelength of fluorescence of the acceptor is denoted λ_{fl} (S_0^A). [b] D(S_1) – A(S_1) denotes the wavenumber difference between the peak wavelength of the first vibronic absorption band of the $S_0 \rightarrow S_1$ transition in the donor and the emission maximum of the acceptor. D(S_2) – A(S_1) denotes the corresponding quantity for the higher-energy transition of the donor, near 260 nm. [c] Φ is the quantum yield of fluorescence. The wavelengths [nm] used to excite of the donor (D) and acceptor (A) groups were as follows: **3**, 420 (D) and 490 (A); **4**, 420 (D) and 490 (A); **7** 385 (D) and 490 (A); **8**, 420 (D) and 490 nm (A); **9**, 420 (D) and 490 (A); and, **10**, 420 (D) and 490 (A).

The fluorescence quantum yields (Φ) of compounds **3**, **4**, and **7**–**10** in chloroform and ethanol were determined (Table 2). In ethanol, Φ takes values between 0.01 and 0.57 and in chloroform between 0.02 and 0.75. The Φ values on were the same whether the donor or the acceptor groups were excited. The absence of a $\Phi(\lambda_{ex})$ dependence suggests nearly complete energy transfer from the donor to the acceptor. The quantum yields measured were always higher when chloroform was used as the solvent than ethanol. Cassette **9** exhibits the highest quantum yield in $CHCl_3$, and **8** exhibits the lowest fluorescence quantum yield in EtOH.

The fluorescence excitation anisotropies of cassettes **9** and **3** provide information about the alignments of excitation and emission transition dipole moments. The excitation anisotropy experiments with **9** in propane-1,2-diol at 262 K (Figure 5), show the anisotropy is about 0.35 for the $S_0 \rightarrow S_1$ transition (450–560 nm). The steady-state fluorescence anisotropy of the compound as a cold glass corresponding to the anthracene $S_0 \rightarrow S_1$ transition (400 nm) is about 0.3. The corresponding limiting fluorescence anisotropies of BODIPY **2** and free anthracene are 0.37[22] and 0.34,[23] respectively. This implies that the overall transition dipoles of cassette **9** are very similar to the polarization of its donor and acceptor constituents. For

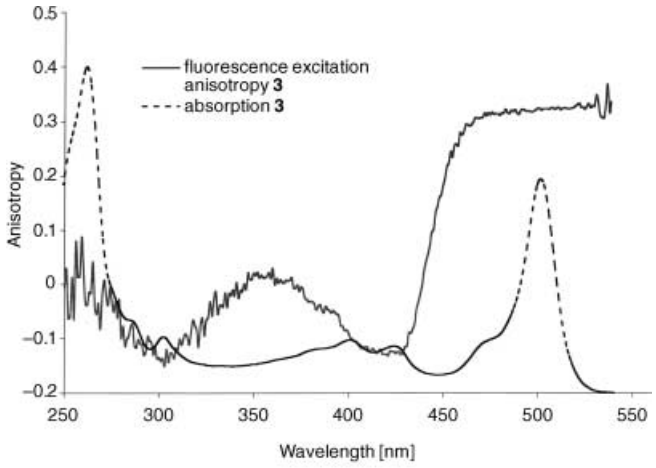

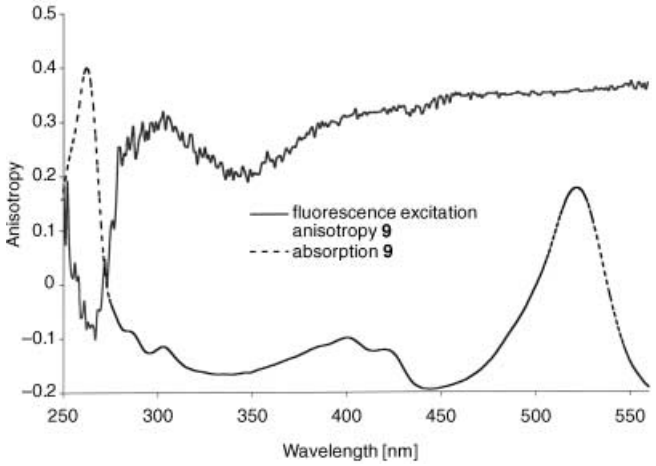

Figure 5. Fluorescence excitation anisotropies and absorption spectra of a) compound **3** and b) compound **9** in propane-1,2-diol at 262 K. The fluorescence emissions were monitored at 570 and 550 nm, respectively.

cassette **3**, the limiting fluorescence anisotropy is about 0.35 in the spectral region arising from the BODIPY $S_0 \rightarrow S_1$ transition (450–560 nm), while it is about -0.15 for the region originating from the anthracene $S_0 \rightarrow S_1$ transition ($\approx$400 nm). The angle (δ) between the absorption and emission transition dipoles is related to the fluorescence steady-state anisotropy (r) through the relationship:

$$r = \frac{r_0}{2}(3\cos^2\delta - 1)$$

where the limiting anisotropy, and r_0 is theoretically $^2/_5$. The blue edge of the $S_0 \rightarrow S_1$ transition band of anthracene is short-axis polarized.[24] It therefore follows from the anisotropy values obtained for the $S_0 \rightarrow S_1$ transition of the BODIPY group in compounds **9** and **3** that the $S_0 \rightarrow S_1$ transition dipole of BODIPY is long-axis polarized. Consequently, energy transfer in cassette **3** cannot be ascribed to point-dipole interactions. The limiting anisotropy of **3** is about zero for the 260 nm absorption of anthracene, but it is significantly smaller (more negative) for **9**. For cassette **9** the transition dipole for the 260 nm absorption of anthracene should be perpendicular to the $S_1 \rightarrow S_0$ emission dipole of the BODIPY fragment, but parallel for system **3**. In cassette **9**, the fluorescence anisotropy is invariant to rotation about the linker axis because of the parallel dipoles, so that the anisotropy is expected to be close to 0.4.[24] The observed value (0.37) is consistent with this reasoning. However, the chemical structure of **3** allows internal rotational freedom of the donor and acceptor about the linker -C_6H_4-CC- component. A random distribution of orientations about the linker axis would give an expected anisotropy value close to 0.1. The lower value observed suggests that the molecular planes of anthracene and BODIPY moieties preferentially adopt non-coplanar orientations possibly in the range 50–60 °C.

The interpretation of the ultrafast spectroscopic measurements required formulation of a generic energy level Scheme for the cassettes. To do this, compounds **4** and **6** were selected because these have very different BODIPY acceptor fragments in the series **3**–**10**, and within that set of compounds it is the acceptor rather than the anthracene-based donor fragments that show the most variation. In the UV spectra of the cassettes (Figure 3) the anthracene component is almost constant and the main differences are with respect to substitution pattern and orientation. The lifetime of the cassettes' lower-lying anthracene level was of primary interest in this study. Figure 6 represents the energy level scheme,

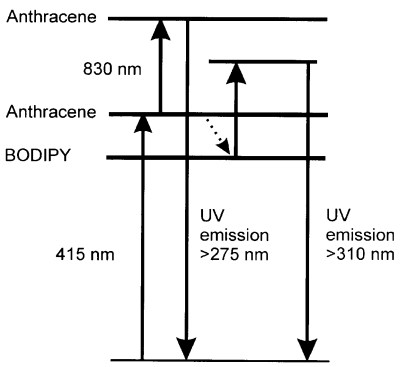

Figure 6. Energy level diagram depicting the anthracene and BODIPY energy levels and showing the origins of different UV emissions in ultrafast two-photon experiments.

showing that synchronization of pulses at 415 and 830 nm leads to high-energy emission, in principle reaching the high-energy limit imposed by the sum of the photon energies ($\approx$275 nm). Delaying the arrival of the 830 nm pulses allows vibrational dephasing and other relaxation processes to occur, so that the accessible region of UV fluorescence is significantly reduced.

Cassette **5** was one of the first prepared, and more sample was available than for some of the other cassettes, so this compound was studied in more depth. The following discussion illustrates the approach used. Figure 7 shows how the ultraviolet emission spectrum depended on the pulse interval for **5** in chloroform. At $t = 0$, when the pulses were synchronized in the sample, emission was observed close to the short-wavelength limit of 275 nm, as expected, in addition to a stronger emission band having a Franck–Condon maximum near 320 nm. This emission band is consistent with observations made by excitation with two photons at 532 nm, and with

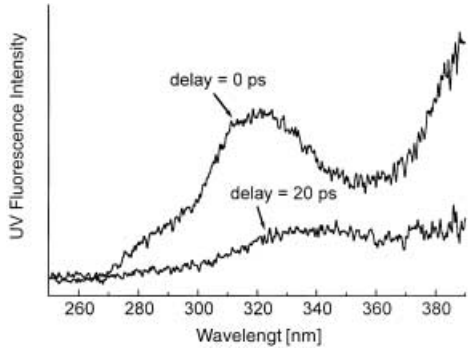

Figure 7. UV emission spectra of cassette **5** resulting from synchronized ($t = 0$) and separated ($t = 20$ ps).

the existence of the abovementioned absorption maximum near 300 nm. In fact, the entire emission spectrum from 275–380 nm is stronger at $t = 0$ than when the pulses are separated. When the 830 nm probe pulses were delayed by 20 ps, the system is seen to have relaxed since the ultraviolet emission is less intense and has shifted to longer wavelengths. This is consistent with relaxation to the BODIPY, from which excitation at 830 nm can generate fluorescence at >310 nm. Therefore, an experiment involving 830 nm probing, with monitoring at <300 nm, should reveal a decay consistent with the energy transfer rate from the anthracene species followed by a more constant signal attributable to vibrationally "hot" lower levels. Time-correlated single-photon counting experiments as well as optically gated fluorescence measurements confirmed that the preliminary relaxation was complete in 50 ps, the only remaining dynamics being associated with nanosecond-scale fluorescence decay.

Figure 8 shows time profile for **5**, which was obtained by scanning the pulse separation, while monitoring the UV fluorescence signal at 300 nm. The data fit a decay time of 550 fs, which we associate with relaxation of the anthracene moiety. The possibility that the UV emission spectrum could depend on the state of relaxation of this complex molecule was real; however, the same decay time against different amounts of background signal was measured over the entire range from 300–390 nm. This experiment detected no significant variation in the apparent dynamics with the sampling wavelength, and we are confident that the signal represents a single relaxation time of the anthracene moiety. Figure 8 also shows, for comparison, a similar decay trace obtained for cassette **6** under the same conditions. That trace, after deconvolution of the instrument response function, showed a relaxation time of only 310 fs.

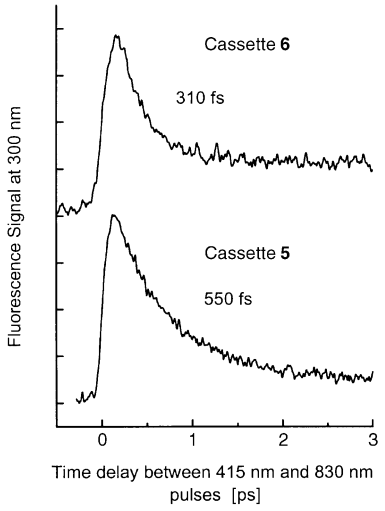

Figure 8. Time profiles resulting from detecting UV emission at 300 nm (see Figure 7) and scanning the time separation of the 415 and 830 nm ultrashort pulses. The relaxation of the anthracene component is caused by energy transfer within the cassettes.

Table 3 shows the collected data from lifetime measurements of the anthracene moiety in a series of BODIPY compounds.[25] The data reveal some significant differences in behavior of the cassettes. Thus, **3**–**6** tend to give stronger UV emission signals, with measurable lifetimes attributable to the anthracene component in the range 300–800 fs (including a solvent effect measured for **5**). The other cassettes tend to give weaker, shorter-lived signals, some of which were apparently decaying within the instrument response profile, which is estimated to be ≈ 150 fs (fwhm).

Table 3. Ultrafast relaxation times of cassettes **3**–**10** in $CHCl_3$ solution as measured by pump-probe spectroscopy.

Compound	S_1 Absorption maximum [nm]	Energy relaxation t [fs]
3	500	320
4	500	490
5	520	550
6	635	310
7	520	<200
8	540	<200
9	525	≈ 200
10	540	≈ 200

Conclusion

In the series of compounds **3**–**10**, two, **8** and **10**, are not truly cassettes, as defined here, since they are fully conjugated systems without an internal twist to break that conjugation. This is reflected in the slightly red-shifted absorption spectra, which also show broader bands than the other compounds in this study. Similarly, the electrochemical studies (Table 1) showed that the degree of donor–acceptor conjugation was greatest for **8**, then **10**.

Compounds **3**–**7** and **9** are true cassettes. X-ray crystallographic studies on single crystals of compounds **7** and **9** revealed the favored conformations of the donor and acceptor fragments, at least in the solid state (Figure 2). In **7**, the anthracene donor and the BODIPY acceptor are directly attached and significant steric interactions prevent the donor and acceptor fragments becoming planar. The corresponding steric effects for compound **9** are evident, but not so severe. Consistent with this, electrochemical studies of **3**, **7**, and **9** revealed that donor acceptor conjugation decreases in the order **3** > **9** > **7**. In studies of absorption and time-resolved

fluorescence spectra, cassette **8** was shown to have different spectroscopic properties from the other compounds in the series; unlike the other cassettes studied, it did not fluoresce significantly when excited at the donor λ_{max}. Quantum yields for the cassettes excited at the donor λ_{max} increased in the order **8** < **7** < **3** < **10** < **4** < **9**. Near complete energy transfer from the donor to the acceptor is suggested by the fact the quantum yields do not vary significantly if the compounds are excited at the donor or acceptor absorbance. The quantum yields measured were always higher when chloroform was used as the solvent than ethanol. Cassette **9** gave the highest fluorescence quantum yield, and **8** the lowest. The average fluorescence lifetimes change in reasonable agreement with changes of the measured quantum yields. Fluorescence emission spectra of the cassettes show maxima varying between 514 and 647 nm. For compounds **3** and **9** it is shown that the $S_0 \rightarrow S_1$ transition dipole of BODIPY group is long-axis polarized. Fluorescence steady-state anisotropy data of cassette **3** suggest that the molecular planes of anthracene and BODIPY are preferentially oriented in a non-coplanar conformation.

The molecules in this study can be grouped into two structural classes. The first, compounds **3**–**6**, have the BODIPY group attached so that its short axis is parallel to the phenylethynyl linker and to the short axis of the anthracene moiety. The substituents on the BODIPY acceptor were varied within this compound set. These cassettes show measurably different relaxation times in the range 300–550 fs (in chloroform). However, despite the wide range of anthracene–BODIPY energy gaps, there was no obvious correlation between the energy gap and the relaxation time. Thus, the lowest absorption bands of **6** are red-shifted relative to the other cassettes in this set, but the relaxation times for all the members fall within the same range. Comparative measurements for **5** in cyclohexane, ethanol and chloroform solutions revealed a variation in lifetime from 500–800 fs, for which ethanol showed the shortest, and cyclohexane solution showed longest decay time. These results reveal the need for caution when interpreting rates in terms of the physical properties of the solute molecule alone.

The second set of molecules **7**–**10** have different separation of the anthracene and BODIPY moieties, and, unlike the first set, have the BODIPY unit attached with its long axis parallel to the linker. All the relaxation times in this group were substantially shorter than for **3**–**6**, in the general range ≈200 fs. The above observations suggest that the orientation of the BODIPY moiety has the greater effect on the relaxation rates of the anthracene subunit than its substitution, or the separation of the two chromophores within this group. The conjugated systems, **8** and **10**, were not exceptional within this group, that is, **7**–**10** all exhibited much faster relaxation dynamics than the first set.

In summary:

- The energy transfer rates measured for cassettes **3**–**6** vary by about a factor of two in chloroform solvent, but no correlation has been established with the structure of the acceptor chromophore;
- all cases where the donor was attached to the long axis of the BODIPY acceptor, as in **7** and **9**, exhibit significantly faster energy transfer than if the donors are coupled to the short axis as in **3**; but
- although the sequence of molecules **7**–**10** was chosen to focus on the possible influence of molecular separation on the transfer rate, the experiments so far employed had insufficient time resolution (≈150 fs) to make a useful comparison.

Experimental Section

General synthetic procedures: Melting points are uncorrected. High field NMR spectra were recorded on Varian Unity Plus (^{1}H at 300 MHz, ^{13}C at 75 MHz, ^{31}P at 121 MHz) or Inova (^{1}H at 500 MHz, ^{13}C at 125 MHz) NMR spectrometers. Chemical shifts are reported in units of ppm relative to the solvent peak ($CDCl_3$: 7.27 ppm for ^{1}H and 77.0 ppm for ^{13}C; D_2O: 4.63 ppm for ^{1}H; [D_6]acetone: 2.04 ppm for ^{1}H and 29.9 ppm for ^{13}C; [D_6]DMSO: 2.50 ppm for ^{1}H and 39.5 ppm for ^{13}C; CD_3OD: 3.30 ppm for ^{1}H and 49.0 ppm for ^{13}C; CD_3CN: 1.93 ppm for ^{1}H and 1.3 ppm for ^{13}C). Mass spectra were obtained from the Mass Spectrometry Applications Laboratory at Texas A&M University using electrospray unless otherwise indicated; the matrix used for the MALDI analyses was 2,4,6-trihydroxyacetophenone. Thin-layer chromatography was performed using silica gel 60 F254 plates. Flash chromatography was performed using silica gel (230–600 mesh). CH_2Cl_2, THF, DMF, triethylamine, and toluene were distilled from appropriate drying agents. Other chemicals were purchased from commercial suppliers and used as received. The product cassettes were made in relatively small quantities, so molar absorptivity and microanalytical data were not obtained.

(2′-Phenylethynyl)-9-anthracene 1: A mixture of 9-bromoanthracene (0.5 g, 1.94 mmol), phenylacetylene (0.42 mL, 3.89 mmol) and [$Pd(PPh_3)_4$] (0.23 g, 0.20 mmol) in triethylamine (2 mL) and THF (5 mL) was stirred at 60 °C under nitrogen for 12 h. The mixture was diluted using EtOAc (20 mL), washed with water, dried ($MgSO_4$) and evaporated to yield crude product. It was purified via silica gel chromatography (hexane/EtOAc 50:1) giving compound **21** (0.45 g, 83 %). M.p. 88–90 °C; R_f 0.54 (hexane/EtOAc 8:1); ^{1}H NMR ($CDCl_3$): δ = 7.51–7.61 (m, 5H), 7.69–7.74 (m, 2H), 7.93 (d, J = 7.5 Hz, 2H), 8.04 (d, J = 8.4 Hz, 2H), 8.41 (s, 1H), 8.82 (d, J = 8.4 Hz, 2H); ^{13}C NMR ($CDCl_3$): δ = 86.4, 100.7, 117.1, 123.6, 125.5, 126.5, 126.6, 127.6, 128.3, 128.4, 128.6, 131.0, 131.6, 132.5; HRMS: m/z: calcd for $C_{22}H_{14}$: 278.1096; found: 278.1093 $[M]^+$.

Cassette 7: nBuLi (1.6 M in hexane, 1.5 mL, 2.10 mmol) at −78 °C under nitrogen was added to a solution of 9-bromoanthracene (0.5 g, 1.95 mmol) in THF (10 mL). After stirring for 15 min at −78 °C, trimethylborate (0.25 mL, 2.10 mmol) was added in one portion. The mixture was allowed to warmed to 25 °C over 30 min, then quenched with dilute HCl. The mixture was extracted with EtOAc (20 mL), washed with water, dried ($MgSO_4$) and evaporated to obtain the crude 9-anthracenylboronic acid that was used without further purification.

9-Anthracenylboronic acid, compound **13** (0.20 g, 0.55 mmol) and [$Pd(PPh_3)_4$] (60 mg, 0.05 mmol) were heated reflux in toluene (10 mL), ethanol (5 mL) and 2 M Na_2CO_3 (2 mL) for 6 h. The mixture was cooled to 25 °C and diluted with EtOAc (20 mL). The mixture was washed with water, dried (Mg_2SO_4) and evaporated to yield crude product that was then purified via silica gel chromatography (hexane/CH_2Cl_2 5:1) to give compound **7** (0.16 g, 71 %). M.p. 255–256 °C; R_f 0.35 (hexane/CH_2Cl_2 1:1); ^{1}H NMR ($CDCl_3$): δ = 1.95 (s, 3H), 2.24 (s, 3H), 2.32 (s, 3H), 2.64 (s, 3H), 6.14 (s, 1H), 7.26 (s, 1H), 7.41–7.52 (m, 4H), 7.76 (d, J = 8.4 Hz, 2H), 8.08 (d, J = 8.1 Hz, 2H), 8.53 (s, 1H); ^{13}C NMR ($CDCl_3$): δ = 10.3, 11.3, 13.3, 14.8, 119.3, 120.3, 125.2, 125.9, 126.2, 127.3, 127.7, 128.0, 128.7, 130.9, 131.4, 132.9, 133.8, 140.3, 141.7, 156.4, 157.5; HRMS: m/z: calcd for $C_{27}H_{23}BF_2N_2$: 424.1922; found: 424.1927 $[M]^+$.

Cassette 8: A mixture of compound 4-(trimethylsilylalkynyl)phenylboronic acid (60 mg, 0.22 mmol), 9-bromoanthracene (85 mg, 0.33 mmol) and [$Pd(PPh_3)_4$] (25 mg, 0.022 mmol) in triethylamine (2 mL) and THF (5 mL) was stirred at 60 °C under nitrogen for 12 h. The mixture was

diluted using EtOAc (20 mL), washed with water, dried ($MgSO_4$) and evaporated to the yield crude product. This was purified via silica gel chromatography (hexane/CH_2Cl_2 3:1) giving compound **8** (60 mg, 61 %). M.p. 300 °C (decomp); R_f (hexane/CH_2Cl_2 1:1); ^{1}H NMR ($CDCl_3$): $\delta = 2.34$ (s, 3H), 2.59 (s, 3H), 2.63 (s, 3H), 2.90 (s, 3H), 6.17 (s, 1H), 7.19 (s, 1H), 7.53–7.58 (m, 2H), 7.61–7.66 (m, 2H), 8.06 (d, $J = 8.7$ Hz, 2H), 8.46 (s, 1H), 8.66 (d, $J = 8.7$ Hz, 2H); ^{13}C NMR ($CDCl_3$): $\delta = 11.1$, 11.4, 13.9, 14.9, 92.5, 93.4, 117.7, 120.1, 120.5, 125.7, 126.6, 127.3, 128.8, 131.2, 132.2, 140.5, 143.0, 149.5, 159.4; MALDI-MS: m/z: calcd for $C_{29}H_{22}BF_2N_2$: 448.19; found: 447.99 $[M]^+$.

Cassette 9: A mixture of compound **17** (20 mg, 0.057 mmol), 9-bromoanthracene (26 mg, 0.10 mmol) and $[Pd(PPh_3)_4]$ (6 mg, 0.05 mmol) in triethylamine (2 mL) and THF (5 mL) was stirred at 60 °C under nitrogen for 12 h. The mixture was diluted using EtOAc (20 mL), washed with water, dried ($MgSO_4$) and evaporated to yield crude product. This was purified via silica gel chromatography (hexane/CH_2Cl_2 5:1) giving compound **9** (12 mg, 40 %). M.p. 221–223 °C; R_f 0.25 (hexane/CH_2Cl_2 1:1); ^{1}H NMR ($CDCl_3$): $\delta = 2.31$ (s, 3H), 2.32 (s, 3H), 2.63 (s, 3H), 2.64 (s, 3H), 6.13 (s, 1H), 7.17 (s, 1H), 7.38 (d, $J = 8.1$ Hz, 2H), 7.54–7.59 (m, 2H), 7.63–7.69 (m, 2H), 7.88 (d, $J = 8.1$ Hz, 2H), 8.07 (d, $J = 8.1$ Hz, 2H), 8.49 (s, 1H), 8.72 (d, $J = 8.1$ Hz, 2H); ^{13}C NMR ($CDCl_3$): $\delta = 10.3$, 11.3, 13.4, 14.8, 86.8, 100.6, 117.2, 119.4, 120.3, 122.2, 125.7, 126.6, 126.7, 127.8, 128.7, 129.8, 131.1, 131.2, 131.7, 132.6, 133.9, 134.0, 137.0, 141.8, 154.3, 157.7; HRMS: m/z: calcd for $C_{35}H_{27}BF_2N_2$: 524.2235; found: 524.2238 $[M]^+$.

Cassette 10: The mixture of compound **13** (200 mg, 0.53 mmol), compound **19** (200 mg, 0.66 mmol) and $[Pd(PPh_3)_4]$ (6 mg, 0.05 mmol) in triethylamine (2 mL) and THF (10 mL) was stirred at 60 °C under nitrogen for 12 h. The mixture was diluted using EtOAc (20 mL), washed with water, dried ($MgSO_4$) and evaporated to yield crude product. This was purified via silica gel chromatography (hexane/CH_2Cl_2 5:1) giving compound **10** (210 mg, 71 %). M.p. 265–266 °C; R_f 0.16 (hexane/CH_2Cl_2 1:1); ^{1}H NMR ($CDCl_3$): $\delta = 2.28$ (s, 3H), 2.39 (s, 3H), 2.57 (s, 3H), 2.70 (s, 3H), 6.11 (s, 1H), 7.10 (s, 1H), 7.50–7.65 (m, 6H), 7.74 (d, $J = 8.7$ Hz, 2H), 8.03 (d, $J = 8.2$ Hz, 2H), 8.45 (s, 1H), 8.65 (d, $J = 8.4$ Hz, 2H); ^{13}C NMR ($CDCl_3$): $\delta = 10.7$, 11.3, 13.6, 14.9, 84.1, 88.2, 95.5, 100.6, 117.0, 120.1, 120.5, 123.1, 123.6, 125.7, 126.7, 128.0, 128.7, 131.2, 131.3, 131.6, 132.2, 132.6, 134.7, 135.2, 140.8, 143.0, 157.6, 159.4; HRMS: m/z: calcd for $C_{37}H_{27}BF_2N_2$: 548.2235; found: 548.2248 $[M]^+$.

Cassette 3: A mixture of compound **19** (0.1 g, 0.29 mmol), 9-bromoanthracene (0.14 g, 0.57 mmol) and $[Pd(PPh_3)_4]$ (33 mg, 0.029 mmol) in triethylamine (2 mL) and THF (5 mL) was stirred at 60 °C under nitrogen for 12 h. The mixture was diluted using EtOAc (20 mL), washed with water, dried ($MgSO_4$) and evaporated to yield crude product. This was purified via silica gel chromatography (hexane/CH_2Cl_2 2:1) giving compound **3** (0.1 g, 66 %). M.p. 260 °C (decomp); R_f 0.28 (hexane/CH_2Cl_2 1:1); ^{1}H NMR ($CDCl_3$): $\delta = 1.55$ (s, 6H), 2.62 (s, 6H), 6.06 (s, 2H), 7.42 (d, $J = 8.1$ Hz, 2H), 7.55–7.60 (m, 2H), 7.64–7.70 (m, 2H), 7.94 (d, $J = 8.4$ Hz, 2H), 8.08 (d, $J = 8.4$ Hz, 2H), 8.51 (s, 1H), 8.71 (d, $J = 8.7$ Hz, 2H); ^{13}C NMR ($CDCl_3$): $\delta = 14.6$, 14.7, 87.7, 99.9, 116.7, 121.4, 124.4, 125.8, 126.6, 126.8, 128.2, 128.4, 128.8, 131.2, 132.3, 132.7, 135.1, 140.8, 143.0, 155.8; HRMS: m/z: calcd for $C_{35}H_{27}BF_2N_2$: 524.2235; found: 524.2242 $[M]^+$.

4-Iodo-3,5-dimethylpyrrole-2-carbaldehyde 12: A mixture of 3,5-dimethylpyrrole-2-carbaldehyde (2.37 g, 19.27 mmol), iodine (5.30 g, 20.88 mmol) and K_2CO_3 (3.93 g, 28.48 mmol) in methanol (50 mL) was stirred under nitrogen at 0 °C for 12 h. The reaction mixture was extracted with Et_2O (100 mL), washed with saturated sodium thiosulfate (50 mL, saturated), dried ($MgSO_4$) and evaporated to yield a crude product. This residue was recrystallized from hexanes/dichloromethane (5:1) to give compound **12** (4.10 g, 85 %). M.p. 161–163 °C; R_f 0.17 (hexanes/EtOAc 4:1); ^{1}H NMR ($CDCl_3$): $\delta = 2.31$ (s, 3H), 2.39 (3H), 9.52 (s, 1H), 10.66 (s, 1H); ^{13}C NMR ($CDCl_3$): $\Delta = 12.6$, 14.3, 72.6, 129.1, 136.8, 140.1, 176.2; HRMS: m/z: calcd for C_7H_8INO: 249.9729; found: 249.9727 $[M]^+$.

BODIPY 13: Phosphorus oxytrichloride (1.00 mL, 11 mmol) was added to a solution of 3,5-dimethylpyrrole (1.02 g, 11 mmol) and iodopyrrole **12** (2.66 g, 11 mmol) in *n*-pentane (5 mL) and CH_2Cl_2 (5 mL) at 0 °C with stirring over 5 min. A red precipitate formed; this was removed by filtration and washed with cold pentane. The filtrates were neutralized with aqueous $Ca(OH)_2$ at 0 °C. The organic layer was extracted by CH_2Cl_2 (100 mL), and washed with water, dried ($MgSO_4$) and evaporated to obtain orange solid (1.52 g). The solid was dissolved into benzene (20 mL) then triethylamine (2 mL, 15.3 mmol) was added, and the reaction mixture was stirred at 25 °C for 10 min. $BF_3 \cdot OEt_2$ (3.2 mL, 25.5 mmol) was added and the mixture was heated to 70 °C for 2 h. The mixture was diluted with EtOAc (100 mL), washed with water, dried ($MgSO_4$) and evaporated to obtain crude product. Purification via flash chromatography on silica gel using hexane/CH_2Cl_2 5:1 gave compound **13** as a orange solid (1.50 g, 36 %). M.p. 212–215 °C; R_f = 0.25 (1:1 hexane/CH_2Cl_2); ^{1}H NMR ($CDCl_3$): $\delta = 2.20$ (s, 3H), 2.24 (s, 3H), 2.54 (s, 3H), 2.57 (s, 1H), 6.10 (s, 1H), 7.05 (s, 1H); ^{13}C NMR ($CDCl_3$): δ = 11.3, 13.6, 14.8, 15.4, 80.5, 120.1, 132.2, 134.1, 142.2, 143.2, 155.3, 159.2; HRMS: m/z: calcd for $C_{13}H_{14}BF_2IN_2$: 374.0263; found: 374.0266 $[M]^+$.

BODIPY 14: A mixture of compound **12** (0.2 g, 0.53 mmol), $[Pd_2(dba)_3] \cdot CHCl_3$ (56 mg, 0.062 mmol), CuI (35 mg, 0.18 mmol), phenol (46 mg, 0.49 mmol) and nBu$_4$NI (0.68 g, 1.85 mmol) was flushed with nitrogen, then, DMF (5 mL) and iPr$_2$Et (0.25 mL) were added, and the mixture was stirred at 25 °C for 5 min. It was then allowed to cool to 0 °C, trimethylsilylacetylene (0.13 mL, 0.93 mmol) was added, and the mixture was stirred at room temperature for 2 h. The mixture was diluted with EtOAc (20 mL), washed with water, dried ($MgSO_4$) and evaporated to yield crude product. This was purified via silica gel chromatography (hexane/EtOAc 15:1) giving compound **14** (0.15 g, 82 %). M.p. 212–213 °C; R_f 0.51 (hexane/EtOAc 4:1); ^{1}H NMR ($CDCl_3$): $\delta = 0.28$ (s, 9H), 2.23 (s, 3H), 2.27 (s, 3H), 2.54 (s, 3H), 2.61 (s, 3H), 6.08 (s, 1H), 7.03 (s, 1H); ^{13}C NMR ($CDCl_3$): δ = 0.1, 10.5, 11.2, 13.3, 14.7, 97.4, 100.5, 113.5, 119.9, 120.6, 131.3, 134.5, 141.5, 142.9, 157.7, 158.9; HRMS: m/z: calcd for $C_{18}H_{23}BF_2N_2Si$: 344.1692; found: 344.1698 $[M]^+$.

BODIPY 15: A solution of trimethylsilylethynyl-BODIPY **14** (0.15 g, 0.44 mmol) in THF (5 mL) was stirred at −78 °C under nitrogen while TBAF (1.0 M in THF, 0.65 mL, 0.65 mmol) was added dropwise over a few minutes. The solution was warmed to 25 °C and stirred at this temperature until TLC analysis indicated completion of reaction (≈30 min). The solution was poured into water (50 mL) and extracted with EtOAc (20 mL). The organic layer was washed with water, dried ($MgSO_4$) and evaporated to yield crude product. This was purified via silica gel chromatography (hexane/EtOAc 15:1) giving compound **15** (60 mg, 51 %). M.p. 173–175 °C; R_f 0.40 (hexane/EtOAc 4:1); ^{1}H NMR ($CDCl_3$): $\delta = 2.25$ (s, 3H), 2.29 (s, 3H), 2.56 (s, 3H), 2.62 (s, 3H), 3.35 (s, 1H), 6.10 (s, 1H), 7.06 (s, 1H); ^{13}C NMR ($CDCl_3$): $\delta = 10.4$, 11.3, 13.2, 14.8, 76.2, 83.0, 112.1, 120.1, 120.7, 131.1, 134.7, 141.8, 143.2, 157.4, 159.4; HRMS: m/z: calcd for $C_{15}H_{15}BF_2N_2$: 272.1296; found: 272.1296 $[M]^+$.

BODIPY 16: nBuLi (1.6 M in hexane, 1 mL, 1.6 mmol) at −78 °C under nitrogen was added to a solution of 4-(trimethylsilylethynyl) iodobenzene (0.3 g, 1.13 mmol) in THF (5 mL). After stirring for 15 min at −78 °C, trimethylborate (0.2 mL, 1.6 mmol) was added in one portion. The mixture was warmed to 25 °C, stirred for 30 min, and quenched with dilute HCl solution. The mixture was extracted with EtOAc (20 mL), washed with water, dried ($MgSO_4$) and evaporated to obtain the crude 4-(trimethylsilylethynyl)phenylboronic acid that was used without further purification.

The boronic acid isolated from above procedure, compound **9** (0.10 g, 0.27 mmol) and $[Pd(PPh_3)_4]$ (30 mg, 0.027 mmol) in toluene (10 mL), ethanol (5 mL) and 2 M Na_2CO_3 (2 mL) were heated under reflux for 5 h. The mixture was cooled to 25 °C and diluted with EtOAc (20 mL). The mixture was washed with water, dried ($MgSO_4$) and evaporated to yield the crude product. This was purified via silica gel chromatography (hexane/CH_2Cl_2 3:1) giving compound **16** (90 mg, 80 %). M.p. 209–210 °C; R_f 0.39 (hexane/CH_2Cl_2 1:1); ^{1}H NMR ($CDCl_3$): $\delta = 0.27$ (s, 9H), 2.23 (s, 3H), 2.30 (s, 3H), 2.53 (s, 3H), 2.59 (s, 3H), 6.11 (s, 1H), 7.14 (s, 1H), 7.21 (d, J = 8.4 Hz, 2H), 7.55 (d, $J = 8.1$ Hz, 2H); ^{13}C NMR ($CDCl_3$): $\delta = 0$, 10.2, 11.3, 13.3, 14.7, 94.8, 104.9, 119.4, 120.3, 121.7, 129.5, 129.6, 131.1, 132.0, 132.2, 133.9, 137.0, 141.7, 154.3, 157.7; HRMS: m/z: calcd for $C_{24}H_{27}BF_2N_2Si$: 420.2005; found: 420.2008 $[M]^+$.

BODIPY 17: A solution of compound **16** (90 mg, 0.21 mmol) in THF (5 mL) was stirred at −78 °C under nitrogen while TBAF (1.0 M in THF, 0.26 mL, 0.26 mmol) was added dropwise over a few minutes. The mixture solution was warmed to 25 °C and stirred until TLC analysis indicated completion of the reaction (≈30 min). The solution was poured into water (50 mL) and extracted with EtOAc (20 mL). The organic layer was washed with water, dried ($MgSO_4$) and evaporated to yield crude product. This was purified via silica gel chromatography (hexane/CH_2Cl_2 4:1) giving compound **17** (50 mg, 68 %). M.p. 204–205 °C; R_f 0.16 (hexane/CH_2Cl_2 1:1); ^{1}H NMR ($CDCl_3$): $\delta = 2.23$ (s, 3H), 2.29 (s, 3H), 2.55 (s, 3H), 2.59 (s, 3H),

3.16 (s, 1H), 6.11 (s, 1H), 7.15 (s, 1H), 7.24 (d, $J = 8.1$ Hz, 2H), 7.58 (d, $J = 8.1$ Hz, 2H); ^{13}C NMR ($CDCl_3$): $\delta = 10.2$, 11.3, 13.3, 14.7, 77.6, 83.5, 119.5, 120.3, 120.6, 129.6, 130.9, 132.2, 132.5, 133.9, 134.3, 136.9, 141.8, 154.1, 157.8; HRMS: m/z: calcd for $C_{21}H_{19}BF_2N_2$: 348.1609; found: 348.1601 $[M]^+$.

Silyldiyne 18: A mixture of 9-ethynylanthracene (200 mg, 0.78 mmol), 4-(trimethylsilylethynyl)iodobenzene (250 mg, 0.86 mmol), $[Pd(PPh_3)_4]$ (8 mg, 0.07 mmol) in triethylamine (2 mL) and THF (10 mL) was stirred at 60 °C under nitrogen for 12 h. The mixture was diluted using EtOAc (20 mL), washed with water, dried ($MgSO_4$) and evaporated to yield crude product. The residue was purified via silica gel chromatography (hexane/CH_2Cl_2 10:1) giving compound **18** (220 mg, 75 %). M.p. 45–46 °C; R_f 0.32 (hexane/CH_2Cl_2 6:1); ^{1}H NMR ($CDCl_3$): $\delta = 0.32$ (s, 9H), 7.49–7.64 (m, 6H), 7.71 (d, $J = 8.4$ Hz, 2H), 8.01 (d, $J = 8.4$ Hz, 2H), 8.42 (s, 1H), 8.63 (d, $J = 8.4$ Hz, 2H); ^{13}C NMR ($CDCl_3$): $\delta = 0$, 88.3, 96.4, 100.3, 104.7, 116.9, 123.0, 123.6, 125.7, 126.6, 126.7, 128.0, 128.7, 131.1, 131.4, 132.0, 132.6; HRMS: m/z: calcd for $C_{27}H_{22}Si$: 374.1491; found: 374.1493 $[M]^+$.

Diyne 19: A solution of compound **7** (220 mg, 0.80 mmol) in THF (10 mL) was stirred at −78 °C under nitrogen while TBAF (1.0 M in THF, 1.2 mL, 1.2 mmol) was added dropwise over several minutes. The mixture solution was warmed to room temp until TLC analysis indicated completion of reaction (≈30 min). The solution was poured into water (50 mL) and extracted with EtOAc (20 mL). The organic layer was washed with water, dried ($MgSO_4$) and evaporated to yield crude product. This was purified via silica gel chromatography (hexane/CH_2Cl_2 10:1) giving compound **19** (200 mg, 75 %). M.p. 45–46 °C; R_f 0.32 (hexane/CH_2Cl_2 6:1); ^{1}H NMR ($CDCl_3$): $\delta = 7.49$–7.64 (m, 6H), 7.73 (d, $J = 8.4$ Hz, 2H), 8.01 (d, $J = 8.4$ Hz, 2H), 8.42 (s, 1H), 8.63 (d, $J = 8.4$ Hz, 2H); ^{13}C NMR ($CDCl_3$): $\delta = 79.1$, 83.3, 88.4, 100.1, 116.8, 122.0, 124.0, 125.7, 126.6, 126.7, 128.1, 128.7, 131.1, 131.4, 132.2, 132.6; HRMS: m/z: calcd for $C_{24}H_{14}$: 302.1096; found: 302.1095 $[M]^+$.

Spectroscopic studies: Spectroscopic grade ethanol was purchased from Kemetyl, chloroform for UV spectroscopy was obtained from Fluka, and synthetic grade propane-1,2-diol from Merck-Schuchardt. Absorption spectra were recorded on a GBC 912 (GBC Scientific Equipment Pty, Ltd, Australia). A SPEX fluorolog 112 instrument (SPEX Industries, Metuchen, NJ, USA) equipped with Glan-Thompson polarizers was used for depolarization experiments. The excitation and emission bandwidths were 5.6 and 2.7 nm, respectively. All fluorescence spectra were corrected. To avoid re-absorption, the maximum absorbance was kept below 0.08. Time-resolved fluorescence experiments were performed on a modified PRA 3000 instrument (PRA Inc., London, Ontario, Canada) using light emitting diodes, NanoLED-01 and NanoLED-05 (IBH, Glasgow, Scotland, UK), for excitation. Excitation wavelengths were isolated through interference filters centered at 440 nm (HBW = 11 nm), 500 nm (HBW = 12 nm) and 520 nm (HBW = 28 nm) (Omega/Saven, Sweden). Fluorescence was observed either through an interference filter at 550 nm (HBW = 40 nm) or a long-pass filter above 610 nm (Schott, Germany).

The fluorescence quantum yield was calculated using the following relationship:

$$\Phi = \Phi\{1 - \exp(-A_{ref}\ln 10)\}n^2 \cdot F(\lambda)\mathrm{d}\lambda[\{1 - \exp(-A\ln 10)\}n_{ref}^2 \cdot F_{ref}(\lambda)\mathrm{d}\lambda]^{-1}$$

where A, n and F denote the absorbance at the excitation wavelength, the refractive index of the medium and the corrected fluorescence spectrum. The reference systems used were perylene in ethanol ($\Phi = 0.92$)[26–28] and 3,3′,4,4′-difluoro-1,3,5,7-tetramethyl-4-borata-3a-azonia-4a-aza-*s*-indacene in methanol ($\Phi = 0.94$).[29]

The concentrations used in the determination of quantum yields were decided upon by the following procedure. To avoid re-absorption, the absorption maximum of BODIPY was chosen to be less than 0.08. Using an estimated molar absorptivity of 60000 $M^{-1}cm^{-1}$, the concentrations were therefore always in the micromolar range.

Ultrafast spectroscopic measurements

General considerations: The time constant for energy transfer from the substituted anthracene moiety to the BODIPY component was measured by ultrafast spectroscopy, by directly probing absorption and fluorescence signals attributable to the anthracene species. Low-quantum-yield emissions from the anthracene chromophores ($\Phi < 5 \times 10^{-5}$) were not readily detected by the usual fluorescence methods, in competition with intrinsic impurities, decomposition products and scattered laser radiation. However, this ultrashort-lived emission can be detected in real time through the application of ultrafast spectroscopy. One approach uses an optical gate, in which some of the emitted fluorescence is mixed with a laser pulse in a nonlinear crystal to generate optical sum-frequency radiation. This signal can then be detected against a much reduced background signal via a monochromator/photomultiplier combination. Such an approach was used by in this laboratory to time-resolve the emission from 5, and provides a reference point for the data presented here.[25] However, intrinsically low signals and sample quantities limited the application of this approach.

Pump-probe techniques provide an alternative way to monitor ultrafast transient events in electronically excited molecules, providing potentially larger signals in the limit of short time resolution. It is well established that, when ultrashort-lived higher-energy electronic states of a molecule are populated by the consecutive absorption of photons from two laser pulses, weak fluorescence can be observed against nearly zero background. This technique was used by Topp and co-workers at 10–30 ps time resolution to time-resolve the singlet lifetimes of weakly fluorescent heterocyclic aromatic molecules and some other species.[30] The present experiments on the anthracene–BODIPY cassettes have excited the anthracene moiety by 415 nm pulses, and subsequently populated an even higher-energy state via 830 nm pulses, leading to fluorescence at $\lambda > 275$ nm. The dependence of the resulting ultraviolet fluorescence intensity on pulse separation provides a record of the dynamics of the intermediate state.

Apparatus: The experiments used a Ti/sapphire laser oscillator/amplifier combination, delivering 200 mW of average power near 830 nm at a repetition rate of 1 kHz. The pulse autocorrelation profile had a width of < 60 fs. Second-harmonic radiation near 415 nm (≈10 mW) was generated in a 1 mm thick BBO crystal, after which the beams were split and then recombined after passing the 830 nm pulses through a variable optical delay line, which was scanned in steps of 1.5 μm (/10 fs increment), and a 620 Hz beam chopper. The experiment used a flowing sample cell ≈1 mm thick, of which fluorescence from the front portion was imaged onto the entrance slit of a double monochromator. The cross-correlation profile of the two pulses, as measured by third-harmonic generation at the surface of a silica slide was ≈90 fs, and the overall cross-correlation profile of the experiment, which was limited by group velocity dispersion in the sample cell, was measured to be ≈150 fs fwhm. The output from a photomultiplier mounted on the back of the monochromator was sampled by a lock-in amplifier synchronized to the beam chopper, and the output was fed to a computer. The experiment involved either a) scanning the fluorescence signal as a function of wavelength at a fixed delay time to generate a transient emission spectrum, or b) scanning the delay line for a fixed detection wavelength to record a time profile.

The results for the above approach were compared with preliminary measurements that had been made earlier for cassettes **4**–**6** by fluorescence upconversion.[25] Since the results agreed closely, we are satisfied that the two-photon approach is indeed measuring the lifetime of the anthracene excited state. This approach was then used for all cassettes because the signal-to-noise ratio was more favorable than for fluorescence upconversion.

Acknowledgement

Use of the TAMU/LBMS-Applications Laboratory directed by Dr. Shane Tichy are acknowledged. Support for this work was provided by The National Institutes of Health (HG 01745) and by The Robert A. Welch Foundation.

[1] J. R. Lakowicz, *Principles of Fluorescence Spectroscopy*, Plenum, New York, **1983**.
[2] L. Stryer, *Annu. Rev. Biochem.* **1978**, *47*, 820.
[3] R. M. Clegg, *Biotechnology* **1995**, *6*, 103.
[4] T. Förster, *Ann. Phys.* **1948**, *2*, 55.
[5] S. Speiser, *Chem. Rev.* **1996**, *96*, 1953.
[6] J. M. Tour, *Chem. Rev.* **1996**, *96*, 537.
[7] R. W. Wagner, J. S. Lindsey, *Pure Appl. Chem.* **1996**, *68*, 1373.

[8] M. S. Vollmer, F. Würthner, F. Effenberger, P. Emele, D. U. Meyer, T. Stümpfig, H. Port, H. C. Wolf, *Chem. Eur. J.* **1998**, *4*, 260.
[9] M. S. Vollmer, F. Effenberger, T. Stümpfig, A. Hartschuh, H. Port, H. C. Wolf, *J. Org. Chem.* **1998**, *63*, 5080.
[10] F. Li, S. I. Yang, Y. Ciringh, J. Seth, C. H. Martin, D. L. Singh, D. Kim, R. R. Birge, D. F. Bocian, D. Holten, J. S. Lindsey, *J. Am. Chem. Soc.* **1998**, *120*, 10001.
[11] R. W. Wagner, J. Seth, S. I. Yang, D. Kim, D. F. Bocian, D. Holten, J. S. Lindsey, *J. Org. Chem.* **1998**, *63*, 5042.
[12] K. Burgess, A. Burghart, J. Chen, C.-W. Wan, in *SPIE BiOS 2000 The International Symposium on Biomedical Optics*, San Jose, CA, **2000**.
[13] A. Burghart, L. H. Thoresen, J. Chen, K. Burgess, F. Bergström, L. B.-Å. Johansson, *Chem. Commun.* **2000**, 2203.
[14] A. Treibs, F.-H. Kreuzer, *Liebigs Ann. Chem.* **1968**, *718*, 208.
[15] E. V. d. Wael, J. A. Pardoen, J. A. v. Koeveringe, J. Lugtenburg, *Recl. Trav. Chim. Pays-Bas* **1977**, *96*, 306.
[16] J. R. Lakowicz, *Principles of Fluorescence Spectroscopy*, 2nd ed., Kluwer Academic/Plenum Publishers, New York, **1999**.
[17] J. Chen, A. Burghart, A. Derecskei-Kovacs, K. Burgess, *J. Org. Chem.* **2000**, *65*, 2900.
[18] N. Miyaura, A. Suzuki, *Chem. Rev.* **1995**, *95*, 2457.
[19] K. Sonogashira, Y. Tohda, N. Hagihara, *Tetrahedron Lett.* **1975**, *16*, 4467.
[20] I. B. Campbell, in *Organocopper Reagents*: *a Practical Approach*, **1994**, pp. 217.
[21] I. B. Berlman, *Handbook of Fluorescence Spectra of Aromatic Molecules*, 2nd ed., Academic Press, London, New York, **1971**.
[22] J. Karolin, L. B.-Å. Johansson, L. Strandberg, T. Ny, *J. Am. Chem. Soc.* **1994**, *116*, 7801.
[23] L. B.-Å. Johansson, J. G. Molotkovsky, L. D. Bergelson, *Chem. Phys. Lipids* **1990**, *53*, 185.
[24] J. Michl, E. W. Thulstrup, *Ber. Bunsenges. Phys. Chem.* **1974**, *78*, 575.
[25] M. F. Wolford, Ph. D. Dissertation thesis, University of Pennsylvania, **2001**.
[26] W. H. Melhuish, *J. Phys. Chem.* **1960**, *64*, 762.
[27] J. N. Demas, G. A. Crosby, *J. Phys. Chem.* **1961**, *65*, 229.
[28] W. Dawson, M. W. Winsor, *J. Phys. Chem.* **1968**, *72*, 3251.
[29] I. A. Johnson, H. C. Kang, R. P. Haugland, *Anal. Biochem.* **1991**, *198*, 228.
[30] H.-B. Lin, M. R. Topp, *Chem. Phys.* **1979**, *36*, 365.

Received: January 22, 2003 [F4754]

